

Spinodal Enhancement of Light Nuclei Yield Ratio in Relativistic Heavy Ion Collisions

Kai-Jia Sun,^{1,*} Wen-Hao Zhou,² Lie-Wen Chen,^{3,†} Che Ming Ko,^{1,‡} Feng Li,^{4,§} Rui Wang,⁵ and Jun Xu^{6,¶}

¹*Cyclotron Institute and Department of Physics and Astronomy,
Texas A&M University, College Station, Texas 77843, USA*

²*Faculty of Science, Xi'an Aeronautical Institute, Xi'an 710077, China*

³*School of Physics and Astronomy, Shanghai Key Laboratory for Particle Physics and Cosmology,
and Key Laboratory for Particle Astrophysics and Cosmology (MOE),
Shanghai Jiao Tong University, Shanghai 200240, China*

⁴*School of Physical Science and Technology, Lanzhou University, Lanzhou, Gansu, 073000, China
Lanzhou Center for Theoretical Physics, Key Laboratory of Theoretical Physics of Gansu Province,
and Frontiers Science Center for Rare Isotopes, Lanzhou University, Lanzhou 730000, China*

⁵*Key Laboratory of Nuclear Physics and Ion-beam Application (MOE),
Institute of Modern Physics, Fudan University, Shanghai 200433, China*

⁶*Shanghai Advanced Research Institute, Chinese Academy of Sciences, Shanghai 201210, China*

(Dated: May 24, 2022)

Using a relativistic transport model to describe the evolution of the quantum chromodynamic matter produced in Au+Au collisions at $\sqrt{s_{NN}} = 3 - 200$ GeV, we study the effect of a first-order phase transition in the equation of state of this matter on the yield ratio $N_t N_p / N_d^2$ (tp/d^2) of produced proton (p), deuteron (d), and triton (t). We find that the large density inhomogeneities generated by the spinodal instability during the first-order phase transition can survive the fast expansion of the subsequent hadronic matter and lead to an enhanced tp/d^2 in central collisions at $\sqrt{s_{NN}} = 3 - 5$ GeV as seen in the experiments by the STAR Collaboration and the E864 Collaboration. However, this enhancement subsides with increasing collision centrality, and the resulting almost flat centrality dependence of tp/d^2 at $\sqrt{s_{NN}} = 3$ GeV can also be used as a signal for the first-order phase transition.

Introduction.— The search for a first-order phase transition and the critical point (CP) in the phase diagram of Quantum Chromodynamics (QCD) is the central goal of the beam energy scan (BES) program in relativistic heavy ion collisions [1, 2]. The transition from the quark-gluon plasma (QGP) to the hadronic matter at vanishing baryon density ρ_B or baryon chemical potential μ_B is known to be a smooth crossover [3, 4]. This phase transition is, however, expected to change to a first-order one at finite μ_B [5–7], resulting in a critical (end)point on the first-order phase transition line in the μ_B - T plane of the QCD phase diagram.

In contrast to the critical point, which is characterized by a divergent correlation length [8, 9], a first-order phase transition is accompanied by a negative compressibility, giving rise to the so-called spinodal instability [10, 11]. The associated non-equilibrium dynamics can lead to inhomogeneities in the density distribution of produced baryons [12, 13]. Results from studies using models based on the hydrodynamic approach [13–16] and the transport approach [17] have shown that the small initial density inhomogeneities in heavy ion collisions are amplified by the spinodal instability when the evolution trajectory of the produced matter traverses the spinodal region of the QCD phase diagram. These enhanced density fluctuations can leave imprints on observables like the event-by-event fluctuations of conserved charges [18, 19], the direct flow of net baryons [20, 21], and the yields of dileptons [17, 22–24], as well as those of light nuclei [14, 25–29].

For light nuclei production, studies based on the coalescence model have shown that the yield ratio $N_t N_p / N_d^2$ (tp/d^2) would be enhanced if large nucleon density fluctuations are present at the late stage of hadronic matter expansion [25, 26]. Experimentally, the preliminary data from heavy ion collisions at both RHIC BES energies [30] and SPS energies [31] have shown possible enhancements and non-monotonic structures in the collision energy dependence of the ratio tp/d^2 , which can not be described by calculations based on transport or hybrid hydrodynamic models without including the effects of spinodal instability and/or long-range correlations. Although it was shown in Ref. [32] that including the spinodal effect in a transport model with a first-order phase transition would lead to an enhancement of tp/d^2 , this study was based on a schematic fireball initial condition for heavy ion collisions at only one collision energy. A systematic study with realistic initial conditions and for various collision energies is needed to extract from the experimental data the equation of state of produced QCD matter.

In the present study, we investigate the effect of spinodal instability in relativistic heavy ion collisions by developing a novel transport model based on an extended Nambu-Jona-Lasinio (NJL) model [33–35] that includes an eight-quark scalar-vector interaction [36] for the partonic matter. This extended NJL model [36] provides a flexible equation of state with the critical temperature T_c ranging from around 40 MeV to 150 MeV, depending on the strength of the scalar-vector interaction, which makes it possible to study realistically the effect of spin-

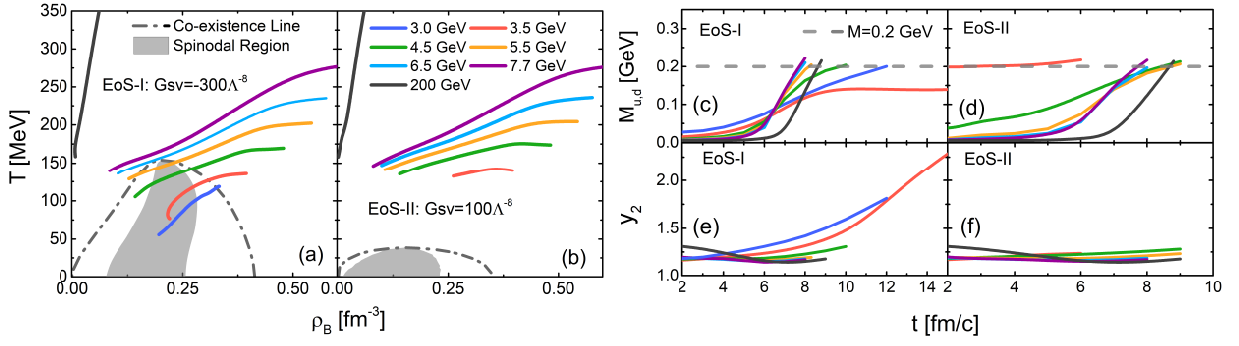


FIG. 1: Left window: Evolution trajectories of the quark matter produced in central Au+Au collisions at $\sqrt{s_{NN}} = 3 - 200$ GeV (solid lines) for EoS-I with $T_c = 154$ MeV and EoS-II with $T_c = 39$ MeV. The shaded regions denote the spinodal region and the dashed-dotted lines denote the co-existence lines. Right window: Time evolution of the in-medium quark mass $M_{u,d}$ (upper panels) and the scaled density moment y_2 (lower panels).

odal instability in Au+Au collisions at $\sqrt{s_{NN}} = 3 - 200$ GeV. With this new approach, we find a clear enhancement of tp/d^2 due to the spinodal instability in heavy ion collisions at $\sqrt{s_{NN}} \approx 3 - 5$ GeV for an equation of state (EoS) with a critical temperature $T_c \gtrsim 80$ MeV. Also, we find that such an enhancement leads to a flat centrality dependence of tp/d^2 at $\sqrt{s_{NN}} = 3$ GeV, which can be used as a signal for the first-order phase transition.

Methods.— For the initial parton distribution in our transport model study, we take it from a multiphase transport (AMPT) model [37]. The time evolution of these partons in the phase space is then described by their motions in the mean-field potentials and mutual scatterings. After converting these quarks to hadrons via the spatial coalescence model in AMPT, which retains the density fluctuations from the partonic matter, the subsequent hadronic rescatterings and decays are further modelled by a relativistic transport (ART) model [38] in AMPT. At the kinetic freeze out when particles cease to scatter, the nucleon coalescence model is employed to evaluate the yields of light nuclei.

The Lagrangian density of the extended three-flavor NJL model with an eight-quark scalar-vector interactions is given by [36]

$$\begin{aligned} \mathcal{L} = & \bar{\psi}(i\gamma^\mu\partial_\mu - \hat{m})\psi + G_S \sum_{a=0}^8 [(\bar{\psi}\lambda^a\psi)^2 + (\bar{\psi}i\gamma_5\lambda^a\psi)^2] \\ & - K \{ [\det[\bar{\psi}(1 + \gamma_5)\psi] + \det[\bar{\psi}(1 - \gamma_5)\psi]] \} \\ & + G_{SV} \left\{ \sum_{a=1}^3 [(\bar{\psi}\lambda^a\psi)^2 + (\bar{\psi}i\gamma_5\lambda^a\psi)^2] \right\} \\ & \times \left\{ \sum_{a=1}^3 [(\bar{\psi}\gamma^\mu\lambda^a\psi)^2 + (\bar{\psi}\gamma_5\gamma^\mu\lambda^a\psi)^2] \right\}, \end{aligned} \quad (1)$$

where $\psi = (u, d, s)^T$ represents the 3-flavor quark fields, λ^a ($a=1, \dots, 8$) is the Gell-Mann matrices, and $\lambda^0 = \sqrt{2/3}I$, and $\hat{m} = \text{diag}(m_u, m_d, m_s)$ is the current quark mass matrix. In the above, G_S is the scalar coupling

constant, K is the coupling constant for the Kobayashi-Maskawa-t'Hooft (KMT) interaction [39] that breaks the $U(1)_A$ symmetry with ‘det’ denoting the determinant in flavor space [35], and G_{SV} is the coupling constant for the scalar-vector (SV) interaction [36]. In the mean-field approximation, the u quark mass is given by the gap equation $M_u = m_u - 4G_S\phi_u + 2K\phi_d\phi_s - 2G_{SV}(\rho_u + \rho_d)^2(\phi_u + \phi_d)$ with $\phi_{i=u,d,s}$ and ρ_i being the quark condensate and net-quark density, respectively. Similar expressions can be obtained for d and s quark masses. In the vacuum or in the chirally restored phase, where $\rho_i = 0$ or $\phi_i = 0$, the scalar-vector interaction does not affect the quark masses. Because of the small current quark masses, the chiral symmetry is only approximately restored at high densities or temperatures. Since the location of the critical point in the QCD phase diagram can be easily changed by varying the value of G_{SV} , as shown in Ref. [36], without affecting the properties of QCD vacuum, the present model is convenient and suitable for investigating the effects of spinodal instability in heavy ion collisions. Due to the non-renormalizability of the NJL model, a momentum cutoff Λ is needed in evaluating the scalar and vector mean fields. For the parameters in this extended NJL model, we use the values $m_u = m_d = 5.5$ MeV, $m_s = 140.7$ MeV, $G_S\Lambda^2 = 1.835$, $K\Lambda^5 = 12.36$, and $\Lambda = 602.3$ MeV [35, 40]. The partonic transport equation derived from the interaction Lagrangian in Eq. (1) is solved by the test particle method [32, 41], with the details given in the supplemental material.

Density fluctuations from the spinodal instability.— The above transport model is used here to study central Au+Au collisions at $\sqrt{s_{NN}} = 3 - 200$ GeV by firstly considering two equations of state with critical temperatures of $T_c = 154$ MeV (EoS-I) and $T_c = 39$ MeV (EoS-II), from setting $G_{SV} = -300\Lambda^{-8}$ and $G_{SV} = 100\Lambda^{-8}$, respectively. In panels (a) and (b) of Fig. 1, the dash-dotted lines depict the co-existence line of the low-density and high-density phases of equal pressure (P), T , and

μ_B . In the shaded region, the quark matter has a negative compressibility $\kappa_T^{-1} = \rho_B(\partial P/\partial \rho_B)_T < 0$ and is unstable against phase decompositions [10]. Each point on the evolution trajectories (solid lines) in the $\rho_B - T$ plane of the phase diagram is obtained from the average temperature and baryon density of the matter in the central volume of $4 \times 4 \times 4 \text{ fm}^3$ weighted by the parton number in each cell of $1 \times 1 \times 1 \text{ fm}^3$. For the temperature in each cell, it is determined by assuming that the energy density and the baryon number density in the rest frame of the cell are the same as those of a thermally equilibrated quark matter described by the present extended NJL model. As shown in panel (a) of Fig. 1, for EoS-I the phase trajectories traverse the spinodal region for collisions at $\sqrt{s_{NN}} < 6.5 \text{ GeV}$. In contrast, for EoS-II the phase trajectories traverse only the crossover region at all collision energies, as shown in panel (b) of Fig. 1.

As the temperature and density of the quark matter decrease during its expansion, the quark masses gradually increase from their current masses in the chirally restored phase to larger masses in the chirally broken phase, as shown in Fig. 1 (c) and (d) for the time evolution of the u and d quark masses $M_{u,d}$. The only exception to this behavior of the quark masses is for EoS-II at $\sqrt{s_{NN}} < 3.5 \text{ GeV}$ where the partonic stage is essentially absent because the chiral symmetry is strongly broken throughout the evolution of the quark matter. Due to the lack of deconfinement transition in the NJL model, we assume in our study that the deconfinement transition coincides with the chiral phase transition as indicated in the lattice QCD calculations for QGP at zero baryon chemical potential [42]. We thus convert quarks to hadrons once the chiral symmetry becomes strongly broken when the average quark mass exceeds 200 MeV , which is about 55% of its constituent mass in vacuum and corresponds to an energy density around 0.26 GeV/fm^3 [43]. With the hadronization carried out via the quark coalescence in the AMPT model, the spinodal effects are then retained during the phase transition and the local baryon density fluctuation is also preserved. We further assume that the lifetime for the quark-hadron mixed-phase does not exceed $t_h = 15 \text{ fm}/c$, i.e., all partons are converted to hadrons before or at $15 \text{ fm}/c$. Prolonging the maximum value of t_h only makes the spinodal effects more pronounced.

To quantify the density fluctuations in the produced matter from heavy ion collisions, we use the second-order scaled density moment y_2 [13], defined as $y_2 = \overline{\rho^2}/\bar{\rho}^2 = [\int d\mathbf{x} \rho(\mathbf{x})][\int d\mathbf{x} \rho^3(\mathbf{x})]/[\int d\mathbf{x} \rho^2(\mathbf{x})]^2$, where $\rho(\mathbf{x})$ denotes the matter density distribution in space. Figure 1 (e) and (f) clearly show that the y_2 can reach a value significantly greater than unity, which is expected from a uniform quark matter distribution, if the evolution trajectory of the produced matter enters the spinodal region of the phase diagram. After converting these quarks to hadrons via the spatial coalescence model in AMPT,

the density fluctuations are smoothly converted from the partonic phase to the hadronic phase. Due to the much larger expansion rate of the subsequent hadronic matter evolution than the hadron rescattering rate needed to maintain local equilibrium, the large density fluctuation is seen to survive at the kinetic freeze-out [32].

Spinodal instability induced enhancement of tp/d^2 .— Although the spatial density fluctuation/correlation in the matter produced from heavy ion collisions cannot be directly measured in experiments, it can affect the production of light (anti-)nuclei [25, 26]. As shown in Refs. [29, 32] based on the nucleon coalescence model, the yield ratio tp/d^2 is approximately given by $y_2/(2\sqrt{3})$ if the density-density correlation length is zero, which then leads to $tp/d^2 \approx 0.29$ in the absence of density fluctuations when $y_2 = 1$. In the nucleon coalescence model for light nuclei production, which has been successfully used in high-energy nuclear collisions [44–48], the formation probabilities of deuteron and triton from a proton-neutron pair and a proton-neutron-neutron triplet, respectively, in the produced hadronic matter at the kinetic freezeout are given by their Wigner functions. The latter are usually taken to be Gaussian, i.e., $W_d = 8g_d \exp\left(-\frac{x^2}{\sigma_d^2} - \sigma_d^2 p^2\right)$ and $W_t = 8^2 g_t \exp\left(-\frac{x^2}{\sigma_t^2} - \frac{\lambda^2}{\sigma_t^2} - \sigma_t^2 p^2 - \sigma_t^2 p_\lambda^2\right)$ with $g_d = 3/4$ ($g_t = 1/4$) being the statistical factor for spin 1/2 proton and neutron to form a spin 1 deuteron (spin 1/2 triton). The size parameters in the Wigner functions are $\sigma_d = \sqrt{4/3} r_d \approx 2.26 \text{ fm}$ and $\sigma_t = r_t = 1.59 \text{ fm}$, respectively, to reproduce the root-mean-squared matter radii of deuteron and triton [32, 49]. The relative coordinates and momenta in W_d and W_t are defined as $\mathbf{x} = (\mathbf{x}_1 - \mathbf{x}_2)/\sqrt{2}$, $\mathbf{p} = (\mathbf{p}_1 - \mathbf{p}_2)/\sqrt{2}$, $\boldsymbol{\lambda} = (\mathbf{x}_1 + \mathbf{x}_2 - 2\mathbf{x}_3)/\sqrt{6}$, and $\mathbf{p}_\lambda = (\mathbf{p}_1 + \mathbf{p}_2 - 2\mathbf{p}_3)/\sqrt{6}$.

Based on the nucleon phase-space distribution functions at the kinetic freeze out from our transport model study of central Au+Au collisions, we have used the above coalescence model to study the collision energy dependence of the yield ratio tp/d^2 . Results obtained from using six different EoSs with critical temperatures of 39, 80, 100, 120, 140, 154 MeV by setting $G_{SV} = 100, -27, -67, -119, -195, -300 \Lambda^{-8}$, respectively, are shown in Fig. 2 by solid lines. For the case of EoS-II with $T_c = 39 \text{ MeV}$, the evolution trajectory of the produced matter in the QCD phase diagram only traverses the crossover region. In this case, the yield ratio tp/d^2 , shown by the blue line, only shows a small increase at low collision energies, which might be due to the change in the volume of produced matter as the collision energy decreases. As T_c increases, the evolution trajectory starts to enter the spinodal unstable region and the enhancement of tp/d^2 at low energies becomes increasingly prominent when $T_c > 80 \text{ MeV}$. A maximum enhancement of tp/d^2 of more than 50% is achieved by using EoS-I with $T_c = 154 \text{ MeV}$. The slight decrease of tp/d^2 at $\sqrt{s_{NN}} < 3.5 \text{ GeV}$

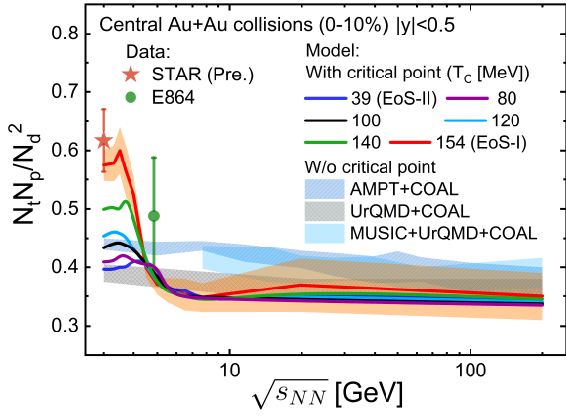


FIG. 2: Collision energy dependence of the yield ratio tp/d^2 from AMPT+COAL [53], UrQMD+COAL [54], and MUSIC+UrQMD+COAL [48] as well as the present transport model study using various values for the critical temperature in the QCD phase diagram. Experimental data are from the STAR Collaboration [50] and the E864 Collaboration [51].

is due to the shortening of the mixed-phase lifetime as seen in Fig. 1. Also shown in Fig. 2 by solid star and solid circle are the experimental data from the STAR Collaboration [50] and the E864 Collaboration [51], respectively, and they are consistent with our theoretical results that include a first-order phase transition in an EoS with $T_c \approx 150$ MeV. In determining the experimental value of tp/d^2 at $\sqrt{s_{NN}} = 4.84$ GeV [51], the yields of light nuclei of atomic number A are obtained by fitting their transverse momentum (p_T) spectra at $p_T/A < 0.3$ GeV with a blast-wave parameterization [52].

Further shown in Fig. 2 are the results from calculations using transport/hydrodynamics approaches without a first-order phase transition in the equation of state together with the coalescence model (COAL) for light nuclei production, i.e., AMPT+COAL [53], UrQMD+COAL [54], and MUSIC+UrQMD+COAL [48]. These studies all give an almost collision energy independent tp/d^2 and fail to explain the enhanced tp/d^2 at $\sqrt{s_{NN}} = 3$ GeV. Similar results have also been obtained in calculations based on more schematic coalescence models [55, 56]. Although allowing in the coalescence model a sequential production of light nuclei according to their decreasing atomic masses can lead to a strong enhancement of tp/d^2 at $\sqrt{s_{NN}} \leq 2.5$ GeV, it has negligible effects at $\sqrt{s_{NN}} \geq 3$ GeV [56]. As to the (preliminary) data of tp/d^2 in heavy ion collisions at higher collision energies of $\sqrt{s_{NN}} > 6$ GeV, such as those at RHIC BES energies [30] and SPS energies [31], the values of tp/d^2 are affected by the weak decay corrections [57, 58] to the proton yield, which needs to be carefully calibrated before comparisons with model predictions are made, and they are therefore not shown in Fig. 2.

Besides the collision energy dependence, the centrality

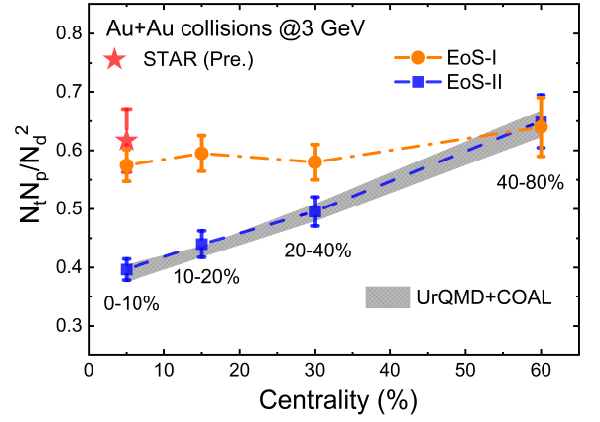


FIG. 3: Centrality dependence of the yield ratio tp/d^2 in Au+Au collisions at $\sqrt{s_{NN}} = 3$ GeV for two different equations of state, with the experimental data taken from the STAR Collaboration [50]. Also shown is the result from the UrQMD+COAL model.

dependence of the yield ratio tp/d^2 in heavy ion collisions can also reveal the occurrence of a first-order phase transition. Because of increasingly shorter lifetime of the produced matter as the collision centrality increases, which limits the development of the spinodal instability during the phase transition, its induced enhancement of tp/d^2 is expected to subside in more peripheral collisions. This effect is clearly seen in Fig. 3, which depicts the centrality dependence of tp/d^2 in Au+Au collisions at $\sqrt{s_{NN}} = 3$ GeV for the two equations of state of EoS-I (solid circles) and EoS-II (solid squares). In the absence of a first-order phase transition, i.e., EoS-II, the yield ratio tp/d^2 is seen to depend linearly on the collision centrality with a slope of 0.44 ± 0.03 , which agrees well with the results from UrQMD+COAL given by the gray band. A similar linear dependence but with a larger slope is obtained for AMPT+COAL (not shown). As shown in Ref. [48] from a study based on the MUSIC+UrQMD+COAL model and also the AMPT+COAL model, such a collision centrality dependence of tp/d^2 is due to the decreasing size of the produced matter with increasing collision centrality. On the other hand, using EoS-I with a first-order phase transition gives an almost flat centrality dependence of tp/d^2 with a slope of 0.09 ± 0.05 that is 5 times smaller, and this is because of the stronger enhancement of tp/d^2 induced by the spinodal instability in more central collisions. A flat centrality dependence of tp/d^2 can thus be used as a distinct signal for a first-order phase transition in relativistic heavy ion collisions and can be tested in RHIC FXT experiments.

We note that the extracted value of $T_c \approx 150$ MeV from our study is larger than those predicted from theoretical approaches based on the functional renormalization method [7] and the Dyson-Schwinger equation [59]. Since the inclusion of hadronic mean-field potential, which is attractive for nucleons, in the hadronic trans-

port is expected to help the survival of density fluctuations during the hadronic matter expansion, it will further enhance the yield ratio tp/d^2 , resulting in the need of an EoS with a smaller T_c to reproduce the experimental data. This effect requires a detailed study in the future.

Conclusion.— Motivated by the fact that finding the signals of a first-order phase transition in relativistic heavy ion collisions would indicate the existence of a critical point and also help determine its location in the QCD phase diagram, we have studied the effect of its associated spinodal instability. Using a novel transport model with a flexible equation of state of variable critical temperatures for relativistic heavy ion collisions, we have demonstrated that the large density inhomogeneities generated from the spinodal instability during the first-order QCD phase transition can significantly enhance the yield ratio tp/d^2 at the kinetic freezeout. We have also found that the spinodal enhancement of tp/d^2 is more prominent for EoS with higher critical temperatures and also in more central collisions. In particular, we have found that the spinodal enhancement of tp/d^2 in central Au+Au collisions at $\sqrt{s_{NN}} \approx 3 - 5$ GeV ($E_{lab} = 3.85 - 12.4$ A GeV) is in accordance with the (preliminary) data from the STAR Collaboration and the E864 Collaboration. Moreover, the almost flat centrality dependence of tp/d^2 at $\sqrt{s_{NN}} = 3$ GeV due to the spinodal instability serves as a cross-check for the occurrence of a first-order phase transition, and this can be tested by precise measurements in RHIC FXT experiments at $\sqrt{s_{NN}} = 3 - 7.7$ GeV and in other experiments at CBM/FAIR, HADES/GSI, CEE/HIAF, NICA/MPD, NA61/SHINE, and J-PARC-HI.

K. J. Sun thanks Xiaofeng Luo, Dingwei Zhang, and Hui Liu for helpful discussions. This work was supported in part by the US Department of Energy under Contract No. DE-SC0015266, the National Natural Science Foundation of China under Grant No. 11922514 and No. 11625521, and National SKA Program of China No. 2020SKA0120300.

* Electronic address: kjsun@tamu.edu

† Electronic address: lwchen@sjtu.edu.cn

‡ Electronic address: ko@comp.tamu.edu

§ Electronic address: fengli@lzu.edu.cn

¶ Electronic address: xujun@zjlab.org.cn;
Kai-Jia Sun and Wen-Hao Zhou contributed equally to this work.

- [1] A. Bzdak, S. Esumi, V. Koch, J. Liao, M. Stephanov, and N. Xu, Phys. Rept. **853**, 1 (2020).
- [2] X. Luo and N. Xu, Nucl. Sci. Tech. **28**, 112 (2017).
- [3] Y. Aoki, G. Endrodi, Z. Fodor, S. D. Katz, and K. K. Szabo, Nature **443**, 675 (2006).
- [4] A. Bazavov et al., Phys. Rev. D **85**, 054503 (2012).
- [5] M. Asakawa and K. Yazaki, Nucl. Phys. A **504**, 668 (1989).

- [6] K. Fukushima and T. Hatsuda, Rept. Prog. Phys. **74**, 014001 (2011).
- [7] W.-J. Fu, J. M. Pawłowski, and F. Rennecke, Phys. Rev. D **101**, 054032 (2020).
- [8] M. A. Stephanov, K. Rajagopal, and E. V. Shuryak, Phys. Rev. D **60**, 114028 (1999).
- [9] M. A. Stephanov, Phys. Rev. Lett. **102**, 032301 (2009).
- [10] P. Chomaz, M. Colonna, and J. Randrup, Phys. Rept. **389**, 263 (2004).
- [11] J. Randrup, Phys. Rev. Lett. **92**, 122301 (2004).
- [12] C. Sasaki, B. Friman, and K. Redlich, Phys. Rev. Lett. **99**, 232301 (2007).
- [13] J. Steinheimer and J. Randrup, Phys. Rev. Lett. **109**, 212301 (2012).
- [14] J. Steinheimer and J. Randrup, Phys. Rev. C **87**, 054903 (2013).
- [15] C. Herold, M. Nahrgang, I. Mishustin, and M. Bleicher, Phys. Rev. C **87**, 014907 (2013).
- [16] C. Herold, M. Nahrgang, I. Mishustin, and M. Bleicher, Nucl. Phys. A **925**, 14 (2014).
- [17] F. Li and C. M. Ko, Phys. Rev. C **95**, 055203 (2017).
- [18] G. Baym and H. Heiselberg, Phys. Lett. B **469**, 7 (1999).
- [19] J. Steinheimer, L. Pang, K. Zhou, V. Koch, J. Randrup, and H. Stoecker, JHEP **12**, 122 (2019).
- [20] H. Stoecker, Nucl. Phys. A **750**, 121 (2005).
- [21] L. Adamczyk et al. (STAR), Phys. Rev. Lett. **112**, 162301 (2014).
- [22] K. Kajantie, J. I. Kapusta, L. D. McLerran, and A. Mekjian, Phys. Rev. D **34**, 2746 (1986).
- [23] R. Rapp and H. van Hees, Phys. Lett. B **753**, 586 (2016).
- [24] F. Seck, T. Galatyuk, A. Mukherjee, R. Rapp, J. Steinheimer, and J. Stroth (2020), 2010.04614.
- [25] K.-J. Sun, L.-W. Chen, C. M. Ko, and Z. Xu, Phys. Lett. **B774**, 103 (2017).
- [26] K.-J. Sun, L.-W. Chen, C. M. Ko, J. Pu, and Z. Xu, Phys. Lett. **B781**, 499 (2018).
- [27] E. Shuryak and J. M. Torres-Rincon, Phys. Rev. C **100**, 024903 (2019).
- [28] E. Shuryak and J. M. Torres-Rincon, Phys. Rev. C **101**, 034914 (2020).
- [29] K.-J. Sun, F. Li, and C. M. Ko, Phys. Lett. B **816**, 136258 (2021).
- [30] D. Zhang (STAR), Nucl. Phys. A **1005**, 121825 (2021).
- [31] T. Anticic et al. (NA49), Phys. Rev. C **94**, 044906 (2016).
- [32] K.-J. Sun, C. M. Ko, F. Li, J. Xu, and L.-W. Chen, Eur. Phys. J. A **57**, 313 (2021).
- [33] Y. Nambu and G. Jona-Lasinio, Phys. Rev. **122**, 345 (1961).
- [34] Y. Nambu and G. Jona-Lasinio, Phys. Rev. **124**, 246 (1961).
- [35] M. Buballa, Phys. Rept. **407**, 205 (2005).
- [36] K.-J. Sun, C.-M. Ko, S. Cao, and F. Li, Phys. Rev. D **103**, 014006 (2021).
- [37] Z.-W. Lin, C. M. Ko, B.-A. Li, B. Zhang, and S. Pal, Phys. Rev. **C72**, 064901 (2005).
- [38] B.-A. Li and C. M. Ko, Phys. Rev. **C52**, 2037 (1995).
- [39] G. 't Hooft, Phys. Rev. D **14**, 3432 (1976), [Erratum: Phys. Rev. D **18**, 2199 (1978)].
- [40] M. F. M. Lutz, S. Klimt, and W. Weise, Nucl. Phys. **A542**, 521 (1992).
- [41] C.-Y. Wong, Phys. Rev. C **25**, 1460 (1982).
- [42] F. Karsch, Lect. Notes Phys. **583**, 209 (2002).
- [43] C. Shen and S. Alzhrani, Phys. Rev. C **102**, 014909 (2020).

- [44] R. Scheibl and U. W. Heinz, Phys. Rev. C **59**, 1585 (1999).
- [45] K.-J. Sun, C. M. Ko, and B. Dönigus, Phys. Lett. B **792**, 132 (2019).
- [46] F. Bellini and A. P. Kalweit, Phys. Rev. C **99**, 054905 (2019).
- [47] W. Zhao, L. Zhu, H. Zheng, C. M. Ko, and H. Song, Phys. Rev. C **98**, 054905 (2018).
- [48] W. Zhao, K.-J. Sun, C. M. Ko, and X. Luo, Phys. Lett. B **820**, 136571 (2021).
- [49] G. Ropke, Phys. Rev. C **79**, 014002 (2009).
- [50] H. Liu (STAR), in *29th International Conference on Ultrarelativistic Nucleus-Nucleus Collisions (Quark Matter 2022) Kraków, Poland, April 4-10* (2022), <https://indico.cern.ch/event/895086/contributions/4717016/>.
- [51] T. A. Armstrong et al. (E864), Phys. Rev. C **61**, 064908 (2000).
- [52] F. Retiere and M. A. Lisa, Phys. Rev. C **70**, 044907 (2004).
- [53] K.-J. Sun and C. M. Ko, Phys. Rev. C **103**, 064909 (2021).
- [54] M. Bleicher et al., J. Phys. G **25**, 1859 (1999).
- [55] H. Liu, D. Zhang, S. He, K.-J. Sun, N. Yu, and X. Luo, Phys. Lett. B **805**, 135452 (2020).
- [56] P. Hillmann, K. Käfer, J. Steinheimer, V. Vovchenko, and M. Bleicher (2021), 2109.05972.
- [57] D. Oliinychenko, C. Shen, and V. Koch, Phys. Rev. C **103**, 034913 (2021).
- [58] X.-Y. Zhao, Y.-T. Feng, F.-L. Shao, R.-Q. Wang, and J. Song (2022), 2201.10354.
- [59] F. Gao, J. Chen, Y.-X. Liu, S.-X. Qin, C. D. Roberts, and S. M. Schmidt, Phys. Rev. D **93**, 094019 (2016).